JCTC Journal of Chemical Theory and Computation

Article

pubs.acs.org/JCTC

Improved Monte Carlo Scheme for Efficient Particle Transfer in Heterogeneous Systems in the Grand Canonical Ensemble: Application to Vapor−Liquid Nucleation

Troy D. Loeffler, Aliasghar Sepehri, and Bin Chen*

Department of Chemistry, Louisiana State University, Baton Rouge, Louisiana 70803, United States

ABSTRACT: Reformulation of existing Monte Carlo algorithms used in the study of grand canonical systems has yielded massive improvements in efficiency. Here we present an energy biasing scheme designed to address targeting issues encountered in particle swap moves using sophisticated algorithms such as the Aggregation-Volume-Bias and Unbonding-Bonding methods. Specifically, this energy biasing scheme allows a particle to be inserted to (or removed from) a region that is more acceptable. As a result, this new method showed a several-fold increase in insertion/removal efficiency in addition to an accelerated rate of convergence for the thermodynamic properties of the system.

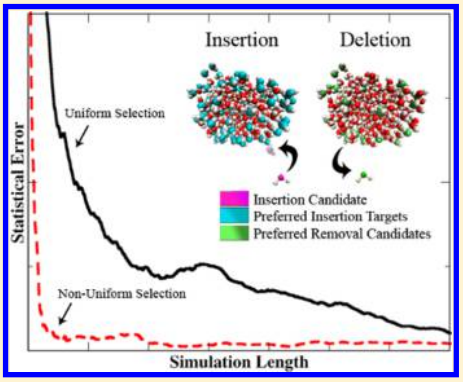

1. INTRODUCTION

The study of nucleation has been a long-standing field of research given its importance to understanding things such as atmospheric nucleation, crystallization, etc.[1−7] Despite its importance, nucleation has traditionally been very difficult to simulate because of the very large time scales that may be required in order to properly observe a nucleation event. For instance, in gas to liquid nucleation the fastest rate that can be observed by the experiments is on the order of 10^{-4} droplet/nm^3/s.[8,9] Even for the simplest system (such as argon modeled by a Lennard-Jones potential) this rate can be barely captured directly by a brute-force dynamical simulation.[9] The rate at which a system will nucleate is tightly linked to the supersaturation ratio and subsequently the ambient gas pressure. At a constant temperature a small change in the supersaturation ratio can lead to a change in the rate of nucleation by several orders of magnitude.[10−12] A natural consequence of this is that if the event a simulator is interested in occurs at a temperature and pressure combination where the nucleation rate is incredibly slow, there is a high chance that it will be impossible to observe this event without the use of specialized methods or conditions. In order to properly observe these events using traditional methods, researchers either include an exceedingly large number of particles to increase the probability of observing an event[9] or arrange the conditions such that the nucleation rate is fast enough to observe within a feasible time frame.[13,14]

As a critical bottleneck encountered by nucleation systems can be often characterized by a large free energy barrier, a common strategy to help speed up the sampling of these systems is to use an artificial bias to drive the system across the free energy barrier. In this regard, techniques such as umbrella sampling[15] or meta-dynamics[16,17] provide very effective ways to allow the system to transverse regions of the phase space with high free energy barriers. The umbrella sampling method is almost trivially implemented into a Monte Carlo simulation given that it only requires the modification of the acceptance rule. However, even with the free energy barrier completely removed via the use of umbrella sampling, the rate at which a simulation can converge the thermodynamic data is still tightly linked to the efficiency of the Monte Carlo moves used to sample phase space. This is especially true when dealing with particle transfer moves, which are another bottleneck for nucleation systems as these moves that are required for cluster growth/destruction can be also time-consuming.

The particle transfer problem is a commonly experienced issue[18,19] when simulating dense or confined systems using the grand canonical or similar ensembles such as the Gibbs ensembles.[20] Among the several techniques introduced in the past,[21−23] the Aggregation-Volume-Bias Monte Carlo (AVBMC) method[24,25] along with its sister algorithm the Unbonding-Bonding (UB) algorithm[26] have both proven very successful at transferring particles into and out of a wide variety of systems.[27−36] While these moves greatly improve the efficiency of particle transfer, a few key issues still remain. For weakly associating systems such as Lennard-Jones, *n*-alkane, etc., the overall acceptance rate of the AVBMC algorithm typically reaches upward of 7−25% depending on the size of the molecule being studied.[37] This is more than sufficient to accurately sample these systems. However, for strongly associating systems such as water or ethanol the acceptance rate for the AVBMC and UB methods typically drops well below 1%.[37] It was presented in ref 37 that the introduction of a

Received: May 20, 2015
Published: July 30, 2015

DOI: 10.1021/acs.jctc.5b00466
J. Chem. Theory Comput. 2015, 11, 4023−4032

basic energy biasing technique can raise the acceptance rate to around 4−6% overall; however, it has since been found that as the number of particles increases the acceptance rate plummets even for this basic energy biasing technique (e.g., to below 1% for a TIP4P system). This problem has in part been linked to the choice of insertion sites by the original algorithms. That is, they use a uniform insertion scheme which simply allows the insertion to occur anywhere in the system despite the fact that the viable insertion sites are located toward the cluster surface. This uniform selection scheme has a glaring flaw that as the cluster grows in size the number of viable insertion sites declines. As a result the odds of randomly picking a valid insertion site via a uniform distribution also decline at a rapid rate (see Section 2.3 for more details). This explains why roughly 100 or more attempted moves are required to generate one acceptable configuration for a moderately dense system of strongly associating molecules. Currently the low acceptance rate of these moves is not a limiting factor when using pairwise models since simulations of reasonable length can feasibly be performed. However, recent efforts have been put forward to study much more complicated water models such as reactive and polarizable models for which these inefficiencies can begin to cause problems.[38−40] Given their increased computational cost, the low acceptance rate may begin to hinder a researcher's ability to study these systems without consuming an unreasonably large amount of computer time. Because of this it is prudent to begin exploring ways to improve the sampling efficiency of current methods.

In this work we examined both the AVBMC and UB methods and found a general solution that can improve the acceptance rate for particle transfer moves and correspondingly the sampling efficiency.

2. METHODOLOGY

2.1. Background. The AVBMC algorithm[24,25] was originally designed to efficiently aggregate molecules using a set of moves that would transfer molecules in and out of another molecule's bound region. This approach had a very similar idea to the UB algorithm developed independently by Wierzchowski and Kofke[26] but differed in how the exchange of particles between the bonding and nonbonding regions is handled. Both methods have very similar moves for the insertion of molecules into a bonded region using the following scheme:

1. Select a molecule from the simulation box to be moved into another molecule's bounding region;
2. Select another molecule to act as the target for the previously selected molecule;
3. Choose a random location within the target molecule's bound region and insert the previously selected molecule.

These two algorithms differ in the unbinding step. Specifically, the following procedure is used in *AVBMC*:

1. Pick a molecule that is currently within another molecule's bound region;
2. Using this target molecule, select one of its neighbors;
3. Move this neighbor out of the selected molecule's bound region to random location within the simulation box.

In UB:

1. Select a molecule that is currently within another molecule's bound region;
2. Move this selected molecule to random location within the simulation box.

The UB algorithm selects a molecule for removal from the bonding region by randomly picking from the global pool of bound molecules, while the AVBMC instead first picks a random molecule from the bound molecules and then chooses one of its neighbors for removal.[25,26] While there seems to be only a subtle difference between the two algorithms, this minor difference can have a profound effect on the detailed balance condition. Since the UB method uses a global approach for the removal step, it must also calculate the global probability of inserting a molecule into the bound region in order to satisfy the detailed balance condition. This includes enumerating all the degenerate insertion pathways that could be used to arrive at the same configuration and their associated probabilities. In contrast the AVBMC method's choice of deletion move allows it to instead rely on the principal of super detailed balance. Since for every possible insertion event there is a corresponding removal via the same path (or target), the degeneracies in the AVBMC's insertion move do not need to be accounted for.

For both methods, the random selection of molecules and also the choice of an insertion position in the bound region were performed by using a simple uniform distribution. However, one downfall of a uniform selection scheme is that when these moves are performed on a cluster that is moderate in size (40+ molecules) the acceptance rate begins to decline proportional to the cluster size (see Section 2.3 for more details). This is naturally explained by the fact that molecules located in the interior of the cluster are saturated with the maximum or near the maximum number of neighbors possible. Subsequently if these molecules are selected as targets for insertion, the move will likely be rejected since there is no space to insert a molecule without some sort of heavy overlap with one of the existing neighbors. For the deletion move if one of these molecules is selected the move will likely be rejected on the grounds that this removal will result in a massive energy penalty. Particles located closer to an interface serve as better sites for both insertion into and removal from the cluster. However, as the cluster increases in size the number of interior particles will increasingly outnumber the particles near the surface. As a result the odds of selecting an interior molecule rapidly outgrow the odds of selecting a particle from the surface. This in turn causes the simulation to waste valuable computational cycles on moves that have close to no hope of ever being accepted. Therefore, it is desirable to avoid poor choices of insertion/removal targets and instead focus on targets that will likely result in a more energetically favorable configuration.

2.2. Derivation of a General Biasing Formula. In order to implement a biasing (or nonuniform) selection scheme, it is important to first derive the general detailed balance rule that will be used. Following the same logic process that was used for the AVBMC algorithm,[25] we can derive a generalized probability for both particle insertion and deletion. For the insertion move, there are two key steps that are generally performed. First, one must select a molecule that will act as the insertion site. Herein we will refer to this as the target molecule. This is typically done by randomly selecting any molecule in the system according to the probability denoted as $P_{\text{Target\_In}}$. Second, once a target molecule has been selected, the coordinates of the new molecule must be generated such that the new molecule lies within the target molecule's bound region. Typically this is done by first randomly inserting an atom of the new molecule within a predefined distance (this distance is usually defined to conform to a cluster criteria[12,41]).

DOI: 10.1021/acs.jctc.5b00466
J. Chem. Theory Comput. 2015, 11, 4023−4032

Once the first atom is inserted the remainder of the molecule is regrown using a method such as Configurational-Bias Monte Carlo (CBMC).[42] The probability of generating this new position within the target molecule's bonded region will be denoted as P_{Bond}. Since AVBMC relies on the super detailed balance condition, one does not need to account for degeneracies. Therefore, the general probability of proposing an insertion move is given by

$$P_{\text{Insert}} = P_{\text{Target\_In}} \cdot P_{\text{Bond}} \tag{1}$$

Next for the removal move first we randomly choose a molecule that has at least one neighbor to act as our target, this probability denoted as $P_{\text{Target\_Out}}$. Second, once a target molecule has been chosen we need to select a molecule from the target molecule's bound region to be removed, i.e., one of the N_{nei} neighbors of the target molecule according to an arbitrary probability denoted as P_{Select}. Therefore, the probability of proposing a move to remove a particle from a given cluster is given by

$$P_{\text{Remove}} = P_{\text{Target\_Out}} \cdot P_{\text{Select}} \tag{2}$$

In contrast, generalizing the UB algorithm requires a little more work since one must derive the global insertion probability in order to properly satisfy the detailed balance condition. To do this we first notice that since the base insertion move is identical to the AVBMC insertion we can argue that the probability of generating this new configuration from a given molecule i is identical, i.e.

$$P_i = P_{i,\text{Target\_In}} \cdot P_{i,\text{Bond}} \tag{3}$$

However, we must account for degeneracies in the insertion step. If the newly inserted molecule rests within the bound regions of more than one molecule, there is now a situation where any one of these molecules could have been used as the target to generate the same identical configuration. For instance if we move a molecule within the bound regions of molecules i and j, we could have first selected molecule i as a target and oriented the new molecule with respect to i or we could have selected molecule j and generated the same configuration by orienting it with respect to j. Because of this there is a multifold degeneracy in the insertion probability that is proportional to the number of neighbors N_{nei} of the newly inserted molecule. Since the probability of using each pathway is independent of all other pathways, we can find the cumulative probability by summing over the probabilities of all possible pathways. For any given insertion move we have N_{nei} pathways, and the total probability to propose this insertion move is given by

$$P_{\text{Insert}} = \sum_{i=1}^{N_{\text{nei}}} P_i = \sum_{i=1}^{N_{\text{nei}}} P_{i,\text{Target\_In}} \cdot P_{i,\text{Bond}} \tag{4}$$

So for every attempted swap move one must determine all potential insertion paths and calculate the probability of each. For instance if the insertion of the first atom of the new molecule is done by randomly generating a point uniformly within a distance r_{max}, then one must search for all insertion sites within this distance. It can be shown if uniform distributions are used, then the original UB insertion probability[26] can be recovered

$$P_{\text{Insert}} = \sum_{i=1}^{N_{\text{nei}}} \frac{1}{N} \cdot \frac{1}{V_{\text{in}}} = \frac{1}{N} \cdot \frac{N_{\text{nei}}}{V_{\text{in}}} \tag{5}$$

where N is the number of particles contained by the cluster, and V_{in} is the volume of the bonded region used for insertion, more specifically a spherical volume centered on the chosen target molecule with a radius of r_{max}. In comparison to the insertion move, the deletion probability is exceedingly simple. All that needs to be done is to simply select a molecule that is in the bound region of one other molecule according to the arbitrary distribution P_{Select}. Therefore, the removal probability is given by

$$P_{\text{Remove}} = P_{\text{Select}} \tag{6}$$

For both methods depending on the ensemble used there of course are other probability terms to consider such as the probability of selecting an unbound molecule from a given simulation box. However, we will primarily focus on the grand canonical ensemble though extending these ideas to other ensembles is fairly straightforward. With these generalized probabilities it is now possible to bias the insertion and removal moves with any arbitrary functional form.

2.3. Choice of Functional Form. As mentioned in the Introduction, it was found after analyzing the original AVBMC algorithm for mid to large sized TIP4P water clusters (with 40+ water molecules) that the majority of molecules that were added to the cluster were added close to the interface (see Figure 1). Therefore, it is theorized that the overall efficiency of

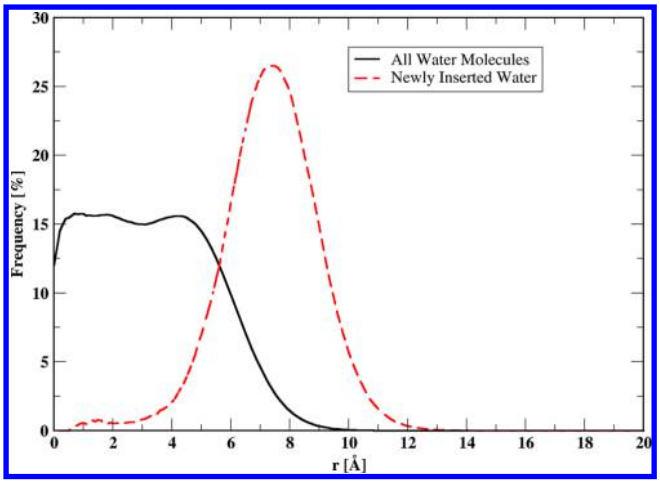

Figure 1. Normalized probability distribution of water oxygen atoms of all molecules in a water cluster containing 45 molecules (black solid line) compared to that of accepted oxygen atom positions for the particle insertion as a function of the distance from the center of mass (dashed red line).

the simulation can be greatly improved if the choice of the insertion site is biased toward the surface of the cluster where there is sufficient empty space. This of course introduces the problem of accurately identifying a molecule that is sufficiently close to the interface. One likely variable that is able to successfully pick out these molecules and will be viable from system to system is the interaction energy of a molecule. A further analysis of the AVBMC algorithm for a TIP4P water system gives credence to this idea as it was found that the molecules which successfully served as a target for insertion tend to have higher energies (see Figure 2). Likewise as shown in previous studies[37] the removal move should also benefit from an energy-based bias to preferentially select particles with the highest energies to be removed from the cluster as these molecules will have the lowest energy penalty for their removal

DOI: 10.1021/acs.jctc.5b00466
J. Chem. Theory Comput. 2015, 11, 4023−4032

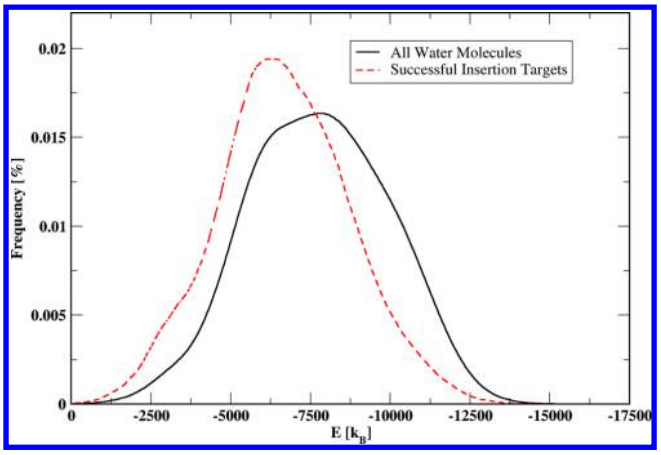

Figure 2. Normalized distribution of the molecular energy over all water molecules at a cluster size of 45 (solid black line) compared to that obtained only for the molecules that successfully acted as a target for the particle insertion (dashed red line) in the original AVBMC algorithm.

and subsequently will have the highest value for the Boltzmann factor in the acceptance probability. Therefore, we have chosen a scheme that attempts to bias the insertion and removal step based on the molecular energy in order to select candidates that are expected to result in successful insertion and removal moves.

For simplicity, the $P_{\text{Target\_in}}$ term in both algorithms was expressed using a similar function form to the one mentioned in ref 37

$$P_{i,\text{Target\_In}} = \frac{e^{\alpha E_i}}{\sum_j e^{\alpha E_j}} \tag{7}$$

where E_i is the total interaction energy of molecule i with all other molecules. It is important to note that the exponential constant α in this case is not chosen to be the usual $\beta = (1/k_B T)$ constant that is common in the Boltzmann weight. Instead α is given as an input parameter that is chosen by the user. This is done because as shown by Figure 2 while the system prefers molecules with higher energy for insertion, there are still some with moderately low energy that can serve as viable insertion targets. Therefore, choosing the exponential constant to be equal to β would bias the system too strongly to the most loosely bound molecules. So to avoid this overbiasing, α is chosen on a system to system basis. In contrast for the removal step selecting a molecule i' according to the exact Boltzmann factor is desirable since this directly corresponds to the change in the energy of the system. Thus, the P_{Select} term is chosen to have the functional form

$$\text{UB: } P_{i',\text{Select}} = \frac{e^{\beta E_{i'}}}{\sum_{j'}^{N} e^{\beta E_{j'}}} \tag{8}$$

$$\text{AVBMC: } P_{i',\text{Select}} = \frac{e^{\beta E_{i'}}}{\sum_{j'}^{N_{i,\text{nei}}} e^{\beta E_{j'}}} \tag{9}$$

For UB this includes all the molecules that can be removed from the cluster while for AVBMC this only includes the neighboring molecules of the target molecule i. This ensures that the highest energy molecules are chosen as removal targets and subsequently have the highest probability of being successfully removed from a cluster. In the UB style algorithm this function selects from all the N bound molecules within the system, while for the AVBMC style this is only done with respect to the neighbors of the target molecule. As mentioned in the AVBMC style algorithm there is the additional $P_{\text{Target\_Out}}$ term to account for that is not found in the UB formulation. The AVBMC style algorithm provides an additional challenge in picking the highest energy molecules for removal since they must be selected indirectly. This was not done in the basic energy biasing scheme mentioned in ref 37 which was subject to the same flaw as the original AVBMC in that if a target molecule is chosen from the center (or a highly dense portion) of the cluster, all of its neighbors will likely be low in energy and the move will be rejected due to the energetic factor. To address this difficulty a variable ϵ_i is introduced which corresponds to the energy value of the highest energy neighbor of molecule i to bias the selection of the target molecule as follows

$$P_{i,\text{Target\_Out}} = \frac{e^{\beta \epsilon_i}}{\sum_j e^{\beta \epsilon_j}} \tag{10}$$

This choice of function ensures that a target molecule with a high energy neighbor will be chosen such that the subsequent molecule selected from its neighbor(s) according to the probability P_{Select} prescribed by eq 9 will have a high chance of being removed from the cluster.

The general acceptance rule for these methods can be constructed using the detail balance condition given by

$$P^{\text{Acc}}_{\text{A}\to\text{B}} \cdot P_{\text{A}\to\text{B}} \cdot P_{\text{A}} = P^{\text{Acc}}_{\text{B}\to\text{A}} \cdot P_{\text{B}\to\text{A}} \cdot P_{\text{B}} \tag{11}$$

where $P^{\text{Acc}}_{\text{A}\to\text{B}}$ is the probability of accepting the transition from state A to state B, $P_{\text{A}\to\text{B}}$ is the probability of proposing the transition from A to B, P_{A} is the probability of being in state A, and all other terms are the equivalent probabilities for the reverse transition. When the appropriate terms are substituted into eq 11, the general acceptance rules in the grand canonical ensemble are given by

$$P^{\text{Acc}}_{\text{Remove}} = \frac{P_{\text{Insert}}}{P_{\text{Remove}}} \cdot e^{-\beta\mu - \beta\Delta E} \tag{12}$$

$$P^{\text{Acc}}_{\text{Insert}} = \frac{P_{\text{Remove}}}{P_{\text{Insert}}} \cdot e^{\beta\mu - \beta\Delta E} \tag{13}$$

where μ is the chemical potential of the ideal gas phase reservoir, and ΔE is the energy difference going from the old to the new state. By substituting all the terms previously listed for each algorithm, the acceptance rules for the energy biased AVBMC and UB algorithms are found.

AVBMC Style:

$$P^{\text{Acc}}_{\text{Remove}} = \frac{\frac{e^{\alpha E_{i,\text{new}}}}{\sum_j^{N-1} e^{\alpha E_{j,\text{new}}}} \cdot \frac{1}{V_{\text{in}}}}{\frac{e^{\beta \epsilon_{i,\text{old}}}}{\sum_j^{N} e^{\beta \epsilon_{j,\text{old}}}} \cdot \frac{e^{\beta E_{i',\text{old}}}}{\sum_{j'}^{N_{i,\text{nei}}} e^{\beta E_{j',\text{old}}}}} \cdot e^{-\beta\mu - \beta\Delta E} \tag{14}$$

$$P^{\text{Acc}}_{\text{Insert}} = \frac{\frac{e^{\beta \epsilon_{i,\text{new}}}}{\sum_j^{N+1} e^{\beta \epsilon_{j,\text{new}}}} \cdot \frac{e^{\beta E_{i',\text{new}}}}{\sum_{j'}^{N_{i,\text{nei}}+1} e^{\beta E_{j',\text{new}}}}}{\frac{e^{\alpha E_{i,\text{old}}}}{\sum_j^{N} e^{\alpha E_{j,\text{old}}}} \cdot \frac{1}{V_{\text{in}}}} \cdot e^{\beta\mu - \beta\Delta E} \tag{15}$$

UB Style:

DOI: 10.1021/acs.jctc.5b00466
J. Chem. Theory Comput. 2015, 11, 4023−4032

$$P_{\text{Remove}}^{\text{Acc}} = \frac{\frac{\sum_i^{N_{\text{nei}}} e^{\alpha E_{i,\text{new}}}}{\sum_j^{N-1} e^{\alpha E_{j,\text{new}}}} \cdot \frac{1}{V_{\text{in}}}}{\frac{e^{\beta E_{i'},\text{old}}}{\sum_{j'}^{N} e^{\beta E_{j'},\text{old}}}} \cdot e^{-\beta\mu - \beta\Delta E} \tag{16}$$

$$P_{\text{Insert}}^{\text{Acc}} = \frac{\frac{e^{\beta E_{i'},\text{new}}}{\sum_{j'}^{N+1} e^{\beta E_{j'},\text{new}}}}{\frac{\sum_i^{N_{\text{nei}}} e^{\alpha E_{i,\text{old}}}}{\sum_j^{N} e^{\alpha E_{j,\text{old}}}} \cdot \frac{1}{V_{\text{in}}}} \cdot e^{\beta\mu - \beta\Delta E} \tag{17}$$

All the energy-related variables listed here can be easily tabulated from the normal energy calculations that are carried out during the course of a simulation. The amount of stored data required by each method is O(N), i.e., linear with respect to the system size and with a proper neighbor list the tabulation of this data increases the computational overhead by a trivial amount. All one needs to do is simply update these tables upon the acceptance of any given Monte Carlo move.

In addition both schemes can be coupled with CBMC in conjunction with multiple insertion.[42−48] In particular, one can generate multiple proposed trial moves to enhance the chance of having one acceptable trial configuration and then use the so-called Rosenbluth weight[48] for trial selection. For this particular application the Rosenbluth weight is given by

$$W = \sum_{m=1}^{M} w_m \tag{18}$$

$$w_m = \frac{e^{-\beta E_m}}{P_{m,\text{Gen}}} \tag{19}$$

$P_{m,\text{Gen}}$ is the probability of generating configuration m, w_m is the Rosenbluth weight of trial m, and E_m is the energy of trial m. For insertion $P_{m,\text{Gen}} = P_{m,\text{Insert}}$, and for removal $P_{m,\text{Gen}} = P_{m,\text{Remove}}$. This follows the same general scheme as CBMC that has previously been used in AVBMC.[32,42] By selecting one of the trials according to the probability $P_m = (w_m/W)$ and computing the Rosebluth weight for the old configuration (W_{old}), one obtains the following acceptance rules:

$$P_{\text{Insert}}^{\text{Acc}} = \frac{W_{\text{new}}}{W_{\text{old}}} \cdot e^{\beta\mu} \tag{20}$$

$$P_{\text{Remove}}^{\text{Acc}} = \frac{W_{\text{new}}}{W_{\text{old}}} \cdot e^{-\beta\mu} \tag{21}$$

It is important to note that for the AVBMC formulation the same target molecule for all trial configurations in a given insertion/removal move was used. This can ensure that the super detail balance condition is not broken by the introduction of the Rosenbluth scheme. In contrast the UB formulation can easily use a different target molecule for each insertion trial since it is not dependent on the super detail balance condition. For small molecules each Rosenbluth trial can be performed by fully growing the molecule (i.e., attempting multiple insertion configurations) although for large chain molecules multiple insertion of the first atom combined with a CBMC regrowth of the rest molecule is more commonly used.

3. SIMULATION DETAILS

All nucleation simulations were carried out using the grand canonical ensemble where a cluster is physically separated from but thermodynamically coupled to an ideal gas-phase reservoir whose chemical potential can be specified by a number density. To compare the accuracy and efficiency of the new scheme to the original algorithms, a cluster simulation of a Lennard-Jones (LJ) and TIP4P Water system was performed for each of the base energy biasing algorithms (denoted as EBias). For the TIP4P system the previously mentioned Rosenbluth scheme was also tested. The LJ simulation was carried out at a reduced temperature of 0.8 and a gas phase number density of $1.1 \times 10^{-2}\ \sigma^{-3}$, while the TIP4P simulations were carried out at 300 K and a gas phase number density of 6×10^{-6} Å^{-3}. For each system the configurational space was sampled using traditional translational moves in addition to particle swaps. Rotational moves were also used for the water system. These different types of moves were performed with equal frequency (e.g., 1/3 for each of the three different move types for the TIP4P system) except where noted explicitly. The maximum displacements for both the translational and rotational (if applicable) moves were adjusted so that 50% of the moves were accepted. For the LJ system clusters up to 200 particles in size were simulated, while for the TIP4P system clusters containing up to 70 water molecules were simulated.

For all simulations the Umbrella Sampling method[15] was used to sample the nucleation free energy of each system. The biasing potential was converged using the method outlined in previous papers via an iterative procedure until uniform sampling is achieved.[12] For all simulations a Stilinger cluster criteria[49] was used. For the LJ simulations a bonding distance of 1.5σ was used, while for the TIP4P simulations a criteria of 4.0 Å was used based on previously published data.[41,50] Any move which would leave a member of the cluster unbound is automatically rejected.

To test the rate of convergence a large simulation (4.5×10^{10} MC moves for the production run) using the original AVBMC algorithm was performed to calculate the free energies of the TIP4P water clusters with high precision. These results were used as the reference to estimate the rate of convergence of each biasing method.

It should be noted that the use of AVBMC or UB for particle transfers combined with the Stillinger cluster criteria avoids the need to define an arbitrary system volume or a simulation cell for the cluster.[12]

4. RESULTS

As shown in Figure 3 all the methods mentioned here were able to correctly reproduce the nucleation free energy profile for the Lennard-Jones system. For both AVBMC and UB, the energy biasing moves showed a massive improvement in the acceptance rate over their uniform counterparts (see Figure 4). In particular, the EBias scheme was able to reach an acceptance rate well above 30% even as the clusters reached larger sizes in comparison to the 10−20% range that was typical of the uniform methods. It was also evident from Figure 4 that the UB method produced a slightly higher acceptance rate than the AVBMC method for this particular system no matter whether the EBias scheme is used or not. When analyzing how the remaining 40−60% of the attempted EBias moves were rejected, it was found that on average roughly 30% were due to energetic reasons, i.e., largely overlaps with the target molecule or one of its neighbors. It was also found that roughly 5−10% of the attempted swap moves were rejected due to the cluster criteria, namely, in the removal step after the deletion of a particle the molecules remaining in the system no longer belong to the same cluster. These numbers would typically

DOI: 10.1021/acs.jctc.5b00466
J. Chem. Theory Comput. 2015, 11, 4023−4032

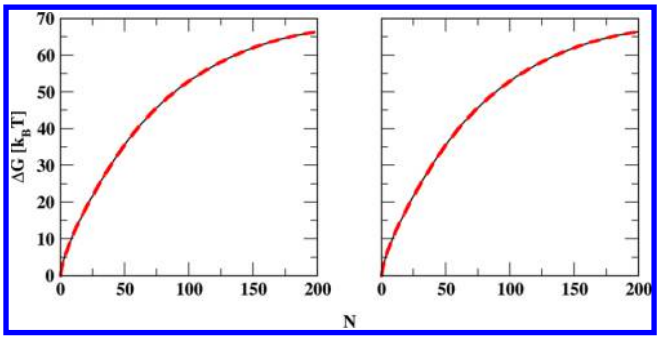

Figure 3. Nucleation free energy results obtained for the Lennard-Jones system as a function of the cluster size using the original uniform selection scheme (black) and the energy-biased scheme (red). The results obtained using the AVBMC-based algorithms are shown on the left, while those obtained using the UB-based methods are shown on the right.

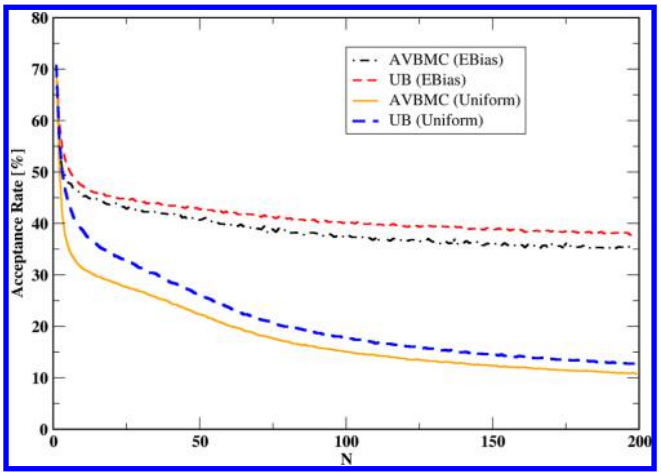

Figure 4. Acceptance rate of the particle transfer move as a function of the cluster size in a Lennard-Jones system obtained using the AVBMC-EBias (dashed-dotted black line), UB-EBias (dashed red line), AVBMC (solid orange line), and UB (dashed blue line) methods.

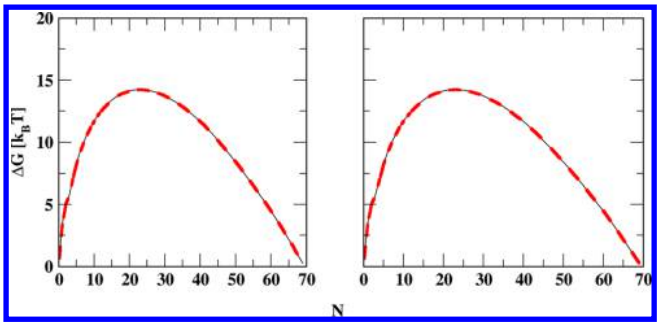

Figure 5. Nucleation free energy results obtained for the TIP4P water system as a function of the cluster size using the original uniform selection scheme (black) and the energy-biased scheme (red). The results obtained using the AVBMC-based algorithms are shown on the left, while those obtained using the UB-based methods are shown on the right.

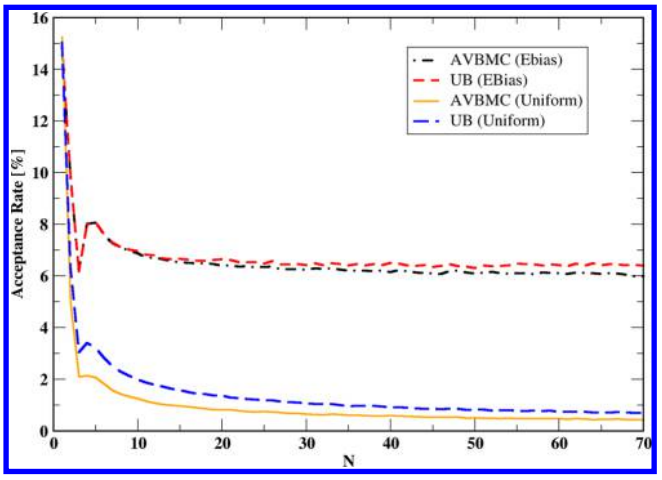

Figure 6. Acceptance rate of the particle transfer move as a function of the cluster size for the TIP4P water system obtained using the AVBMC-EBias (dashed-dotted black line), UB-EBias (dashed red line), AVBMC (solid orange line), and UB (dashed blue line) methods.

fluctuate depending on the cluster size. For smaller clusters the rejection rate due to the cluster criteria was typically higher, while the rejection rate due to energetic factors would be higher for larger cluster sizes. Since the EBias schemes brought the acceptance rate to nearly 50%, it was not deemed necessary to implement the Rosenbluth sampling scheme for this system.

Similarly the method was able to correctly reproduce the free energy curve of the TIP4P system (see Figure 5). While not as dramatic as the Lennard-Jones system, for this water system the EBias scheme showed a modest improvement over the uniform sampling scheme (see Figure 6). As the cluster grew beyond 30 water molecules in size the uniform scheme showed a sharp decline in the acceptance rate, falling below 1%. In contrast the EBias scheme maintained an acceptance rate well above 5% even as the cluster grew larger in size. The overall acceptance rates were around 6.5%. For comparison purposes an equivalent run was performed using the EBias scheme implemented in ref 37, and it was found that the overall acceptance rate was approximately 4.2% for the same conditions.

It became apparent that while the smarter selection of target molecules improved the overall acceptance rate, there was still a very large number of moves that were rejected compared to the LJ case because the newly inserted water molecule was not aligned so that it could properly hydrogen bond with the surrounding cluster members. The Rosenbluth scheme described in Section 2.3 can be used to deal with this issue. In order to provide a fair one to one comparison with the combined Rosenbluth/EBias method (called EBias-Rosen), the same Rosenbluth sampling method was also implemented with the uniform insertion scheme (denoted as Uniform-Rosen). As shown in Figure 7, the EBias-Rosen method resulted in a remarkable improvement in the acceptance rate far exceeding that achieved by Uniform-Rosen. It was also found that EBias-Rosen's overall acceptance rate scales very well with the number of trials (see Figure 8). For both the EBias-enhanced AVBMC and UB algorithms, the introduction of the Rosenbluth sampling greatly improved the acceptance rate from 5 to 7% to anywhere between 20 and 35% depending on the number of trials used. It was found that scaling beyond 32 Rosenbluth trials was not desirable given that the acceptance rate only increased by 2−5% from 32 to 64 trials, while simultaneously the computational overhead nearly doubled. In stark contrast to the EBias-Rosen scheme the Uniform-Rosen method displayed very minor improvements on the absolute magnitude of the acceptance rate. Even for an exceedingly large number of trials the Uniform-Rosen methods did not reach

DOI: 10.1021/acs.jctc.5b00466
J. Chem. Theory Comput. 2015, 11, 4023−4032

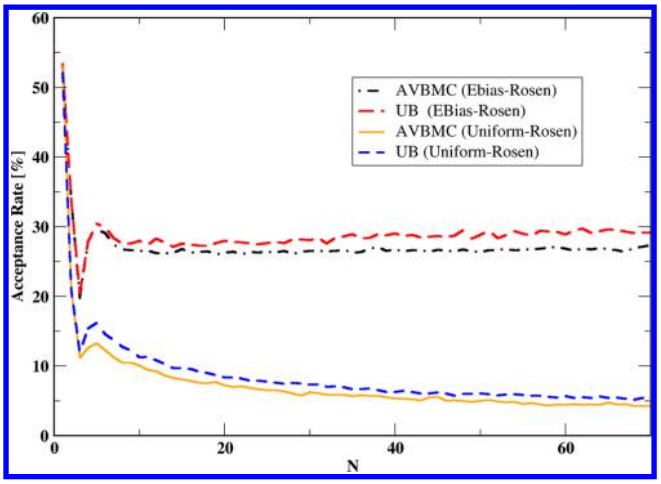

Figure 7. Acceptance rate of the particle transfer move as a function of the cluster size for the TIP4P water system obtained using the Rosenbluth coupled version of each algorithm with 32 trials, including AVBMC-EBias (dotted blue line), UB-EBias (dashed-dotted purple line), AVBMC (solid black line), and UB (dashed red line).

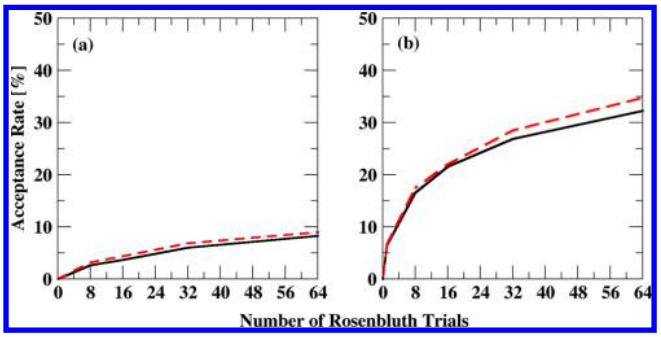

Figure 8. Acceptance rate of the particle transfer move as a function of the number of Rosenbluth trials using AVBMC (black lines) and UB (red dashed lines). The results obtained using the standard algorithms are shown on the left, while those obtained using the Ebias enhanced methods are shown on the right.

10% in the acceptance rate. The acceptance rate of the Uniform-Rosen methods much like the standard Uniform methods showed a massive drop toward larger clusters. Thus, one can conclude that the Rosenbluth scheme alone is not sufficient to improve the acceptance rate as the system size grows.

An increase in the acceptance rate does not necessarily guarantee that the rate of convergence of the system's thermodynamic properties is improved. To evaluate the convergence rate, two sets of simulations were performed, and these two differ in terms of the input biasing potentials used by umbrella sampling. One starts with unconverged values and the other with well-converged ones. The number of Rosenbluth trials used for the Ebias-Rosen methods were set to 32. For the case using initially unconverged biasing potentials, the starting input biases (see Figure 9) were chosen such that each cluster would have a chance of being sampled so the free energies of all cluster sizes can be evaluated directly from their sampling frequencies. This was done to ensure that the speed-up was due to the method and not to outside factors such as the choice of the extrapolation method.[51] As shown in Figure 10, the original uniform methods were found to take 4 iterations to accurately converge the free energy curve within a reasonable statistical error, and before that the statistical error

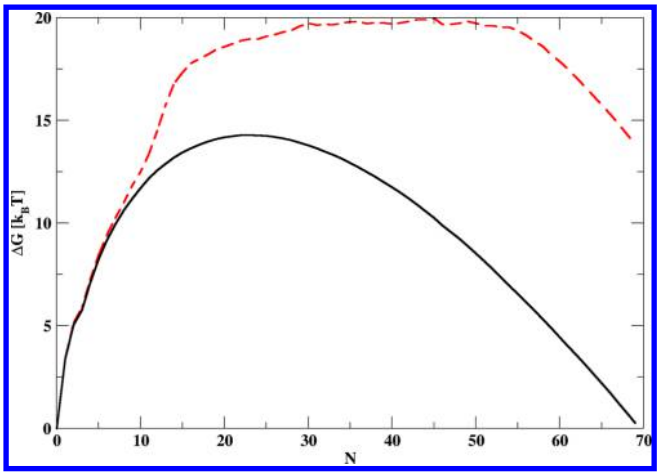

Figure 9. Two sets of input biasing potentials used in the convergence evaluation. The solid black curve is the fully converged profile obtained from a very long simulation run, while the dashed red curve is the unconverged one used as the starting point for the iterations.

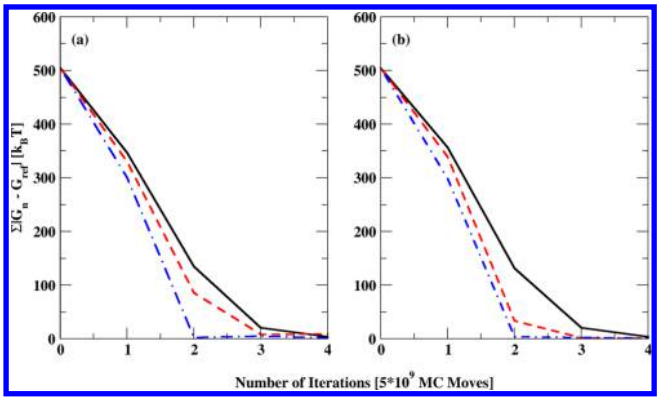

Figure 10. Sum of the absolute error of the nucleation free energy over all cluster sizes as a function of the number of simulation iterations for each of the different methods, including the standard method (solid black line), the Ebias method (dashed red line), and the Ebias-Rosen method (dashed-dotted blue line). The results obtained using the AVBMC-based algorithms are shown on the left, while those obtained using the UB-based methods are shown on the right.

showed a fairly linear decrease with respect to the number of iterations. The EBias scheme needs 3 iterations, and for each step the relative error was smaller than the uniform algorithm. Lastly the EBias-Rosen schemes were able to reach the convergence within 2 iterations. For the second set of simulations using the well-converged biasing potentials, the free energies and also the errors were analyzed every 2×10^6 MC moves. As shown in Figure 11, the EBias and EBias-Rosen methods showed a significant increase in computational efficiency, up to an order of magnitude (measured by the number of moves needed to obtain high-quality free energies) compared to the original uniform selection schemes. It is evident that the increase in the acceptance rate due to these nonuniform algorithms does indeed result in a faster sampling of the conformational space and correspondingly a faster convergence of the thermodynamic properties of the system.

When comparing the overall differences between UB and AVBMC, it was found that on average the various UB methods showed a higher acceptance rate by 1−4% compared to their AVBMC counterparts. This difference can largely be attributed to the two-step proposal scheme in the AVBMC algorithm. A

DOI: 10.1021/acs.jctc.5b00466
J. Chem. Theory Comput. 2015, 11, 4023−4032

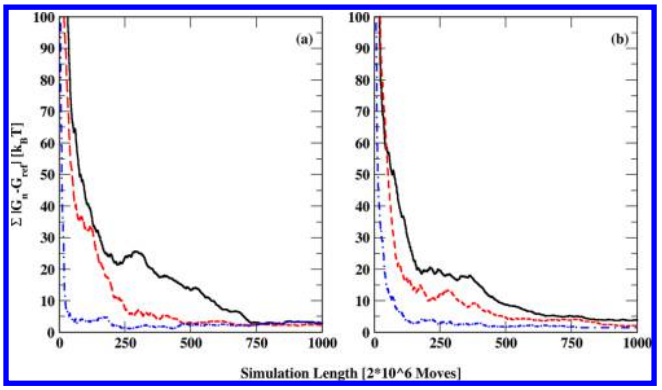

Figure 11. Sum of the absolute error of the nucleation free energy over all cluster sizes as a function of the number of Monte Carlo moves using the standard method (solid black line), the Ebias method (dashed red line), and the Ebias-Rosen method (dashed-dotted blue line). The results obtained using the AVBMC-based algorithms are shown on the left, while those obtained using the UB-based methods are shown on the right.

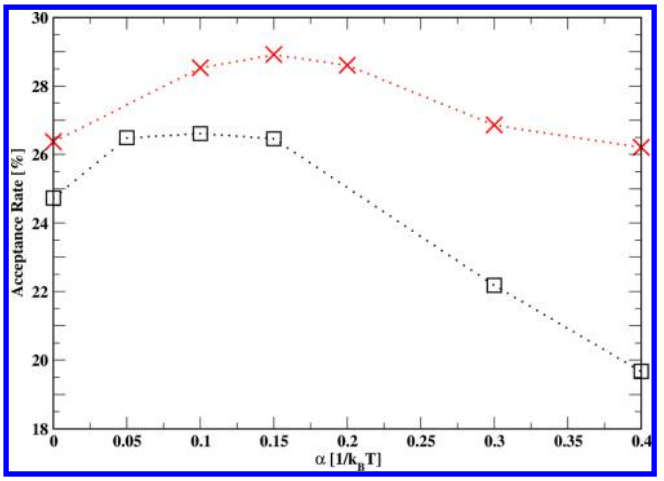

Figure 12. Acceptance rate of the particle transfer move as a function of the α parameter for the Ebias-Rosen AVBMC (black squares) and the Ebias-Rosen UB method (red ×'s).

two-step selection scheme is inherently more prone to selecting a bad candidate for removal because either a poor choice of a target molecule or a poor choice of the subsequent neighbor selection can give this result. Conceptually if there is a 99% chance of generating a good target and a 99% chance of selecting a good neighbor, the cumulative probability of choosing a proper candidate is around 98% or that there is now a 2% instead of 1% chance of selecting a poor candidate. In addition in the uniform case, the two-step algorithm was more likely be rejected due to the cluster criteria. It was found that for the water system UB had a 1.0% rejection rate due to the cluster criteria compared to 1.7% for AVBMC. The two-step selection scheme in the uniform case is statistically more likely to select particles that have a higher number of neighbors (e.g., a particle with two neighbors has two pathways that it can be selected by while a particle with one neighbor only has one pathway to be selected by), whereas in UB all molecules have the same probability of being selected for deletion. However, for the EBias enhanced versions the cluster criteria was no longer an issue. Both algorithms had a similar criteria-induced rejection rate of around 0.05% for the water system.

While UB consistently outperforms AVBMC, the implementation of biased UB algorithms is more complicated since it requires additional efforts to take into account the degeneracy-related terms which arise when different pathways can lead to the same configurational change during a particle swap move. In the schemes presented here the increase in algorithmic complexity was reasonable; however, if any sort of orientational bias is introduced (e.g., the insertion of the first bead is biased using an arbitrary orientation angle with respect to the target molecule), the orientation probability must be calculated with respect to all degenerate insertion sites for the UB formalism, whereas in AVBMC this needs to be done only for the chosen insertion target. It should be also pointed out that the optimal value of α (a parameter used for the nonuniform selection of the target molecule for insertion) varied significantly between these two formalisms. As shown in Figure 12, for the TIP4P water system the acceptance rate peaked at an α value between 0.05β and 0.1β for AVBMC vs a value between 0.1β and 0.15β for UB. Beyond 0.15β both algorithms begin to see a decline in the acceptance rate. In this region, the system begins to suffer from overbiasing or that the probability overwhelmingly favors the highest energy molecules. However, as previously shown in Figure 2 this neglects a large population of molecules which can still serve as viable insertion sites. While this affects both algorithms the UB variation of the EBias-Rosen displayed a lower sensitivity to the choice of α due to its globalized sampling capabilities. Even though the probability of selecting a moderately high energy molecule was low (often below 5% at an α value of 0.3β) over the course of 32 Rosenbluth trials the odds of generating at least one trial using these molecules were high enough that they could be included in the Rosenbluth weight. In contrast the AVBMC due to its restriction to a single target site for all Rosenbluth trials is significantly more sensitive to the choice of the target molecule given that a poor target selection will doom the majority of the Rosenbluth trials. The results reported above were obtained using an optimal α value corresponding to each of these two types of methods (i.e., 0.1β for AVBMC and 0.15β for UB). For the TIP4P system, additional simulations were performed by changing the frequency of the swap moves from 1/3 to either 1/6 or 1/2 while splitting the rest of the moves evenly between translations and rotations to evaluate the influence of this parameter on the rate of convergence. It was found that the use of a lower frequency of the swap moves (i.e., 1/6) led to a slower convergence, while the use of a higher frequency of the swap moves (i.e., 1/2) produced mixed results.

As noted, the extension of these methods into other ensembles such as the Canonical or Gibbs ensembles can be achieved by following the formulations in the original AVBMC and UB papers.[25,26] These methods are expected to work for bulk phase systems given that a few additional optimizations are included for bulk systems. For instance since a bulk system has many more interactions compared to a cluster system, using the full energy calculation to compute the Rosenbluth weight could prove to be far too costly. However, this can be solved by weighting according to a local subset of the interactions instead of all the interactions in the system, as what has been done in the dual-cutoff CBMC.[52] While the Rosenbluth sampling assists in overcoming rejections due to the poor choice of an insertion orientation, a more direct approach would be to bias the generation of the trial orientation to the expected distribution, similar to the idea that was proposed recently for the conformational sampling of chain molecules.[53]

DOI: 10.1021/acs.jctc.5b00466
J. Chem. Theory Comput. 2015, 11, 4023−4032

5. CONCLUSION

In conclusion, we have demonstrated that by selectively biasing the choice of insertion site as well as the selection of molecules for removal, the AVBMC and UB swap moves can have their sampling efficiency greatly improved over the standard uniform algorithms. While these methods require some additional bookkeeping, the overall increase in the acceptance rate is promising. In addition there still remains room to further improve the sampling efficiency of the presented algorithms.

AUTHOR INFORMATION

Corresponding Author

*E-mail: binchen@lsu.edu.

Notes

The authors declare no competing financial interest.

ACKNOWLEDGMENTS

We would like to thank the Louisiana Optical Network (LONI) and Louisiana State High Powered Computing Center (LSU-HPC) for supplying us with the computational resources needed to carry out these simulations. In addition we would like to thank the National Science Foundation (CHE-1052015 and EPS-1003897) for providing us with financial support.

REFERENCES

(1) Kulmala, M.; Riipinen, I.; Sipilä, M.; Manninen, H. E.; Petäjä, T.; Junninen, H.; Maso, M. D.; Mordas, G.; Mirme, A.; Vana, M.; Hirsikko, A.; Laakso, L.; Harrison, R. M.; Hanson, I.; Leung, C.; Lehtinen, K. E. J.; Kerminen, V.-M. Toward Direct Measurement of Atmospheric Nucleation. *Science* **2007**, *318* (5847), 89−92.

(2) He, G.; Dahl, T.; Veis, A.; George, A. Nucleation of apatite crystals in vitro by self-assembled dentin matrix protein 1. *Nat. Mater.* **2003**, *2* (8), 552−558.

(3) Blow, D. M.; Chayen, N. E.; Lloyd, L. F.; Saridakis, E. Control of nucleation of protein crystals. *Protein Sci.* **1994**, *3* (10), 1638−1643.

(4) Aastuen, D. J. W.; Clark, N. A.; Cotter, L. K.; Ackerson, B. J. Nucleation and Growth of Colloidal Crystals. *Phys. Rev. Lett.* **1986**, *57* (14), 1733−1736.

(5) Korhonen, H.; Kerminen, V.-M.; Kokkola, H.; Lehtinen, K. E. J. Estimating atmospheric nucleation rates from size distribution measurements: Analytical equations for the case of size dependent growth rates. *J. Aerosol Sci.* **2014**, *69* (0), 13−20.

(6) Jokinen, T.; Sarnela, N.; Sipilä, M.; Junninen, H.; Lehtipalo, K.; Duplissy, J.; CLOUD Collaboration. Molecular steps of neutral sulfuric acid and dimethylamine nucleation in CLOUD. *AIP Conf. Proc.* **2013**, *1527* (1), 302−305.

(7) Lupi, L.; Kastelowitz, N.; Molinero, V. Vapor deposition of water on graphitic surfaces: Formation of amorphous ice, bilayer ice, ice I, and liquid water. *J. Chem. Phys.* **2014**, *141* (18), 18C508.

(8) Sinha, S.; Bhabhe, A.; Laksmono, H.; Wölk, J.; Strey, R.; Wyslouzil, B. Argon nucleation in a cryogenic supersonic nozzle. *J. Chem. Phys.* **2010**, *132* (6), 064304.

(9) Angélil, R.; Diemand, J.; Tanaka, K. K.; Tanaka, H. Properties of liquid clusters in large-scale molecular dynamics nucleation simulations. *J. Chem. Phys.* **2014**, *140* (7), 074303.

(10) Hale, B. N. Temperature dependence of homogeneous nucleation rates for water: Near equivalence of the empirical fit of Wölk and Strey, and the scaled nucleation model. *J. Chem. Phys.* **2005**, *122* (20), 204509.

(11) Brus, D.; Ždímal, V.; Uchtmann, H. Homogeneous nucleation rate measurements in supersaturated water vapor II. *J. Chem. Phys.* **2009**, *131* (7), 074507.

(12) Chen, B.; Siepmann, J. I.; Oh, K. J.; Klein, M. L. Aggregation-volume-bias Monte Carlo simulations of vapor-liquid nucleation barriers for Lennard-Jonesium. *J. Chem. Phys.* **2001**, *115* (23), 10903−10913.

(13) Tanaka, K. K.; Kawano, A.; Tanaka, H. Molecular dynamics simulations of the nucleation of water: Determining the sticking probability and formation energy of a cluster. *J. Chem. Phys.* **2014**, *140* (11), 114302.

(14) Wedekind, J.; Wölk, J.; Reguera, D.; Strey, R. Nucleation rate isotherms of argon from molecular dynamics simulations. *J. Chem. Phys.* **2007**, *127* (15), 154515.

(15) Torrie, G. M.; Valleau, J. P. Nonphysical sampling distributions in Monte Carlo free-energy estimation: Umbrella sampling. *J. Comput. Phys.* **1977**, *23* (2), 187−199.

(16) Laio, A.; Parrinello, M. Escaping free-energy minima. *Proc. Natl. Acad. Sci. U. S. A.* **2002**, *99* (20), 12562−12566.

(17) Ensing, B.; De Vivo, M.; Liu, Z.; Moore, P.; Klein, M. L. Metadynamics as a Tool for Exploring Free Energy Landscapes of Chemical Reactions. *Acc. Chem. Res.* **2006**, *39* (2), 73−81.

(18) Shi, W.; Maginn, E. J. Atomistic Simulation of the Absorption of Carbon Dioxide and Water in the Ionic Liquid 1-n-Hexyl-3-methylimidazolium Bis(trifluoromethylsulfonyl)imide ([hmim]-[Tf2N]. *J. Phys. Chem. B* **2008**, *112* (7), 2045−2055.

(19) Woo, H.-J.; Dinner, A. R.; Roux, B. Grand canonical Monte Carlo simulations of water in protein environments. *J. Chem. Phys.* **2004**, *121* (13), 6392−6400.

(20) Panagiotopoulos, A. Z. Direct determination of phase coexistence properties of fluids by Monte Carlo simulation in a new ensemble. *Mol. Phys.* **1987**, *61* (4), 813−826.

(21) Mezei, M. A cavity-biased (T, V, μ) Monte Carlo method for the computer simulation of fluids. *Mol. Phys.* **1980**, *40* (4), 901−906.

(22) Busch, N. A.; Wertheim, M. S.; Chiew, Y. C.; Yarmush, M. L. A Monte Carlo method for simulating associating fluids. *J. Chem. Phys.* **1994**, *101* (4), 3147−3156.

(23) Brennan, J. K. Cavity-bias sampling in reaction ensemble Monte Carlo simulations. *Mol. Phys.* **2005**, *103* (19), 2647−2654.

(24) Chen, B.; Siepmann, J. I. A Novel Monte Carlo Algorithm for Simulating Strongly Associating Fluids: Applications to Water, Hydrogen Fluoride, and Acetic Acid. *J. Phys. Chem. B* **2000**, *104* (36), 8725−8734.

(25) Chen, B.; Siepmann, J. I. Improving the Efficiency of the Aggregation−Volume−Bias Monte Carlo Algorithm. *J. Phys. Chem. B* **2001**, *105* (45), 11275−11282.

(26) Wierzchowski, S.; Kofke, D. A. A general-purpose biasing scheme for Monte Carlo simulation of associating fluids. *J. Chem. Phys.* **2001**, *114* (20), 8752−8762.

(27) Wierzchowski, S.; Kofke, D. A. UB association bias algorithm applied to the simulation of hydrogen fluoride. *Fluid Phase Equilib.* **2002**, *194−197* (0), 249−256.

(28) Loeffler, T. D.; Henderson, D. E.; Chen, B. Vapor−liquid nucleation in two dimensions: On the intriguing sign switch of the errors of the classical nucleation theory. *J. Chem. Phys.* **2012**, *137* (19), 194304.

(29) Loeffler, T. D.; Chen, B. Surface induced nucleation of a Lennard-Jones system on an implicit surface at sub-freezing temperatures: A comparison with the classical nucleation theory. *J. Chem. Phys.* **2013**, *139* (23), 234707.

(30) Keasler, S. J.; Kim, H.; Chen, B. Sign preference in ion-induced nucleation: Contributions to the free energy barrier. *J. Chem. Phys.* **2012**, *137* (17), 174308.

(31) Naresh, D. J.; Singh, J. K. Virial coefficients and inversion curve of simple and associating fluids. *Fluid Phase Equilib.* **2009**, *279* (1), 47−55.

(32) Chen, B.; Siepmann, J. I.; Oh, K. J.; Klein, M. L. Simulating vapor−liquid nucleation of n-alkanes. *J. Chem. Phys.* **2002**, *116* (10), 4317−4329.

(33) Khan, S.; Singh, J. K. Prewetting transitions of one site associating fluids. *J. Chem. Phys.* **2010**, *132* (14), 144501.

(34) Kamath, G.; Cao, F.; Potoff, J. J. An Improved Force Field for the Prediction of the Vapor−Liquid Equilibria for Carboxylic Acids. *J. Phys. Chem. B* **2004**, *108* (37), 14130−14136.

DOI: 10.1021/acs.jctc.5b00466
J. Chem. Theory Comput. 2015, 11, 4023−4032

(35) Mehrabi, A. R.; Sahimi, M. Cluster conformations and multipole distributions in ionic fluids. I. Two-dimensional systems of mobile ions. *J. Chem. Phys.* **2008**, *128* (23), 234503.
(36) Birkett, G. R.; Do, D. D. Simulation Study of Water Adsorption on Carbon Black: The Effect of Graphite Water Interaction Strength. *J. Phys. Chem. C* **2007**, *111* (15), 5735−5742.
(37) Nellas, R. B.; McKenzie, M. E.; Chen, B. Probing the Nucleation Mechanism for the Binary n-Nonane/1-Alcohol Series with Atomistic Simulations. *J. Phys. Chem. B* **2006**, *110* (37), 18619−18628.
(38) Kumar, R.; Knight, C.; Wick, C. D.; Chen, B. Bringing Reactivity to the Aggregation-Volume-Bias Monte Carlo Based Simulation Framework: Water Nucleation Induced by a Reactive Proton. *J. Phys. Chem. B* **2015**, *119* (29), 9068−9075.
(39) Keasler, S. J.; Kim, H.; Chen, B. Ion-Induced Nucleation: The Importance of Ionic Polarizability. *J. Phys. Chem. A* **2010**, *114* (13), 4595−4600.
(40) Wu, Y.; Chen, H.; Wang, F.; Paesani, F.; Voth, G. A. An Improved Multistate Empirical Valence Bond Model for Aqueous Proton Solvation and Transport†. *J. Phys. Chem. B* **2008**, *112* (2), 467−482.
(41) Chen, B.; Siepmann, J. I.; Klein, M. L. Simulating Vapor−Liquid Nucleation of Water: A Combined Histogram-Reweighting and Aggregation-Volume-Bias Monte Carlo Investigation for Fixed-Charge and Polarizable Models. *J. Phys. Chem. A* **2005**, *109* (6), 1137−1145.
(42) Siepmann, J. I.; Frenkel, D. Configurational bias Monte Carlo: a new sampling scheme for flexible chains. *Mol. Phys.* **1992**, *75* (1), 59−70.
(43) Escobedo, F. A.; de Pablo, J. J. Extended continuum configurational bias Monte Carlo methods for simulation of flexible molecules. *J. Chem. Phys.* **1995**, *102* (6), 2636−2652.
(44) Martin, M. G.; Siepmann, J. I. Novel Configurational-Bias Monte Carlo Method for Branched Molecules. Transferable Potentials for Phase Equilibria. 2. United-Atom Description of Branched Alkanes. *J. Phys. Chem. B* **1999**, *103* (21), 4508−4517.
(45) Wick, C. D.; Siepmann, J. I. Self-Adapting Fixed-End-Point Configurational-Bias Monte Carlo Method for the Regrowth of Interior Segments of Chain Molecules with Strong Intramolecular Interactions. *Macromolecules* **2000**, *33* (19), 7207−7218.
(46) Shelley, J. C.; Patey, G. N. A configuration bias Monte Carlo method for water. *J. Chem. Phys.* **1995**, *102* (19), 7656−7663.
(47) Vendruscolo, M. Modified configurational bias Monte Carlo method for simulation of polymer systems. *J. Chem. Phys.* **1997**, *106* (7), 2970−2976.
(48) Rosenbluth, M. N.; Rosenbluth, A. W. Monte Carlo Calculation of the Average Extension of Molecular Chains. *J. Chem. Phys.* **1955**, *23* (2), 356−359.
(49) Stillinger, F. H. Rigorous Basis of the Frenkel-Band Theory of Association Equilibrium. *J. Chem. Phys.* **1963**, *38* (7), 1486−1494.
(50) Jorgensen, W. L.; Chandrasekhar, J.; Madura, J. D.; Impey, R. W.; Klein, M. L. Comparison of simple potential functions for simulating liquid water. *J. Chem. Phys.* **1983**, *79* (2), 926−935.
(51) Chen, B.; Kim, H.; Keasler, S. J.; Nellas, R. B. An Aggregation-Volume-Bias Monte Carlo Investigation on the Condensation of a Lennard-Jones Vapor below the Triple Point and Crystal Nucleation in Cluster Systems: An In-Depth Evaluation of the Classical Nucleation Theory. *J. Phys. Chem. B* **2008**, *112* (13), 4067−4078.
(52) Vlugt, T. J. H.; Martin, M. G.; Smit, B.; Siepmann, J. I.; Krishna, R. Improving the efficiency of the configurational-bias Monte Carlo algorithm. *Mol. Phys.* **1998**, *94* (4), 727−733.
(53) Sepehri, A.; Loeffler, T. D.; Chen, B. Improving the efficiency of configurational-bias Monte Carlo: A density-guided method for generating bending angle trials for linear and branched molecules. *J. Chem. Phys.* **2014**, *141* (7), 074102.

DOI: 10.1021/acs.jctc.5b00466
J. Chem. Theory Comput. 2015, 11, 4023−4032